Appl. Phys. A (2014) 117:767–771
DOI 10.1007/s00339-014-8643-5

Applied Physics A
Materials Science & Processing

RAPID COMMUNICATION

Thermal and microstructural investigation of Cu–Al–Mn–Mg shape memory alloys

Canan Aksu Canbay · Soner Ozgen ·
Zuhal Karagoz Genc

Received: 21 May 2014 / Accepted: 22 July 2014 / Published online: 31 July 2014

Abstract There are many studies to improve the properties of Cu–Al–Mn shape memory alloys, such as high transformation temperatures, ductility and workability. Most of them have been performed by adding a quaternary component to the alloy. In this study, the effect of trace Mg addition on transformation temperatures and microstructures of three different quaternary Cu–Al–Mn–Mg alloys has been investigated using thermal analysis, optical microscopy and XRD techniques. The transformation temperatures are within the range of 120–180 °C, and they have not changed significantly on decreasing the Mn content, replacing with Mg. The fine precipitates have been observed in the alloys with the Mg content up to 1.64 at%. Calculated entropy change and XRD analysis reveal that the alloys with high Al content have mainly 18R-type structure which could be responsible for good ductility and workability.

1 Introduction

Cu–Al–Mn alloys are well-known types of shape memory alloys introduced to technological use. In general, Cu–Al alloys quenched from high temperatures at which the alloy is stable in β phase field exhibit thermoelastic martensitic transformation which is important to obtain the shape memory effect (SME) [1]. In order to prevent the decomposition of β and β_1 phases to α and γ_2 during quenching, which they interfere the martensitic transformation kinetics and therefore shape memory properties, another alloying element is added into Cu–Al binary alloys, such as Zn [2–5], Ni [6–10], Mn [11–16], Be [17–19] or Ag [20, 21]. By adding Mn into Cu–Al alloys, it has been gained the magnetic properties, and the excellent ductility and large super elasticity strain are obtained by controlling their grain size and texture [16]. Therefore, ternary Cu–Al–Mn shape memory alloys are the most popular one among Cu–Al-based high-temperature memory alloys which are candidates to use in high-technology applications [16, 22, 23]. However, the performance of these alloys still depends on some questions to be solved [24]: how to improve the unsuitable ductility and workability of the polycrystalline alloys resulting from the coarse grain and how to control the metastability of both the parent and martensite phases which result in complicated ageing effects?

The workability of these alloys depends significantly on the Al ratio. When the Al ratio is decreased, the workability of the alloy increases in important scale. However, in the case of Al content less than or equal to 16 at%, the SME is lost dramatically due to the forming of disordered A2 structures in the alloys [25]. In this case, in order to preserve the SME, the β phase region can be broadened by increasing Mn ratio. The transformation temperatures of the order–disorder transitions also depend strongly on the Al ratio rather than on the Mn, and their values decrease with decreasing amount of Al [26]. The optimum composition which has a good SME and a high workability at the same time is confirmed to be a Cu—17 at% Al—10 at% Mn [23]. In the same report, it has also been noted that the onset temperatures of martensitic transition, M_s, can be adjusted by changing the Mn content from 10 to 13 at%.

C. A. Canbay (✉) · S. Ozgen
Faculty of Science, Department of Physics, Firat University, Elazig, Turkey
e-mail: caksu@firat.edu.tr

Z. K. Genc
Faculty of Engineering, Department of Materials Engineering, Adiyaman University, Adiyaman, Turkey

Present study has been aimed to produce a new type of quaternary shape memory alloys by adding trace amount of Mg into the Cu–Al–Mn alloys. The new alloys that should work at elevated temperatures have a good SME and a high workability. For this purpose, without reducing the Al content which makes the SME worse, the Mn content was replaced with Mg element, because recently Mg has been added to many alloys in a trace amount to get a good workability [27–29]. In this way, three different quaternary alloys were produced here.

2 Experimental

The alloys used in the present study were produced by arc melting under an argon atmosphere using the powder elements with high purity of 99.99 %. Chemical compositions of the alloys produced here are given in Table 1. The samples were cut from the cast ingot. The specimens were solution treated at 750 °C in the β phase region for 1 h and quenched in iced-brine water. The chemical compositions of the alloys were determined by LEO evo 40 Model energy dispersive X-ray (EDX) analyses. The specimens were polished for the EDX analysis but not etched in order to avoid the possible influence of chemical etching on the EDX results. The XRD measurements were carried out in a Rigaku RadB-DMAX II diffractometer using Cu-K$_\alpha$ ($\lambda = 1.5405$ Å) radiation. After the EDX and X-ray analysis, the specimens were etched using a solution that consisted of 5 g (FeCl$_3$-6H$_2$O)-96 ml methanol with 20 ml HCl. The structures of the specimens were characterized under a Nikon MA 200 Model optic microscope. The thermodynamic characteristics of the specimens were determined by Shimadzu DSC-60A differential scanning calorimeter (DSC). DSC measurements were carried out from room temperature to 250 °C with 10 °C/min heating and cooling rates. The TG/DTA (Shimadzu TA-60 WS) measurements were performed from room temperature to 1000 °C at a heating rate of 20 °C/min to observe the phase transitions at high temperatures.

3 Results and Discussions

It has been reported that the cold workability of the Cu–Al–Mn shape memory alloys is suppressed by adding the Mg higher than 2 at% to an alloy having the Cu/Al ratio of 2.77 and 4.85 % Mn in atomic percentages (converted from Cu$_{81.5}$–Al$_{12.5}$–Mn$_{5.0}$–Mg$_1$ in wt%) [5]. Also, it is well known that the decomposition temperature of β$_1$ in these alloys increases with increasing Mn content and the addition of 1 % Mn into Cu–Al binary alloys increases the decomposition temperature by about 30 °C. Therefore, Mn is known as a useful stabilizing element for β$_1$ phase which is important to obtain good SME [11]. For these reasons, in our study the Mg content of the alloys was not increased above 2 at% and it was aimed to keep the ratio of Cu/Al constant at 2.67, replacing the Mn content with Mg.

Table 1 Chemical compositions of the alloys in atomic and weight (in parentheses) percentages

Alloy	Cu	Al	Mn	Mg
MG1	69.54 (82.85)	25.84 (13.07)	3.42 (3.52)	1.21 (0.55)
MG2	69.76 (83.23)	26.07 (13.21)	2.85 (2.94)	1.32 (0.60)
MG3	69.70 (83.36)	26.17 (13.29)	2.50 (2.58)	1.64 (0.75)

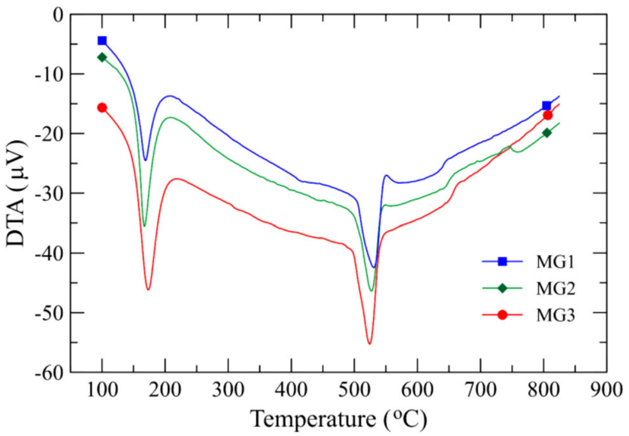

Fig. 1 DTA curves obtained at heating rate of 20 °C/min

Figure 1 shows the DTA curves obtained with heating rate of 20 °C/min for three alloys. On heating, the first endothermic peaks belong to the transformations from martensite to austenite phase, which occur in a temperature range of 150–200 °C, while the second peaks appearing between 500 and 550 °C temperatures are related to the order–disorder solid reactions which are defined as the transition from ordered β$_1$ (DO$_3$- or L2$_1$-type structure) to β (B2) phase [26, 30–33]. Also it has been seen that the small exothermic energy changes occur at temperatures close to 650 °C which are related to the transitions from B2 to A2 [25, 26]. The alloys studied here have not any peaks related to magnetic transitions because the alloys with Mn content lower than 8 at% do not exhibit remarkable magnetic properties [26, 32].

The DSC curves obtained with heating/cooling rate of 10 °C/min for three alloys are shown in Fig. 2. The machine-derived temperatures of the transformations and the enthalpy differences between martensitic and austenitic conditions are also given in Table 2. From the DSC curves and the values of transition temperatures, one can see that the addition of a trace amount of Mg into the Cu–Al–Mn alloy is not much effective on the transformation temperatures, except for a slight systematic increase in the reverse transformation

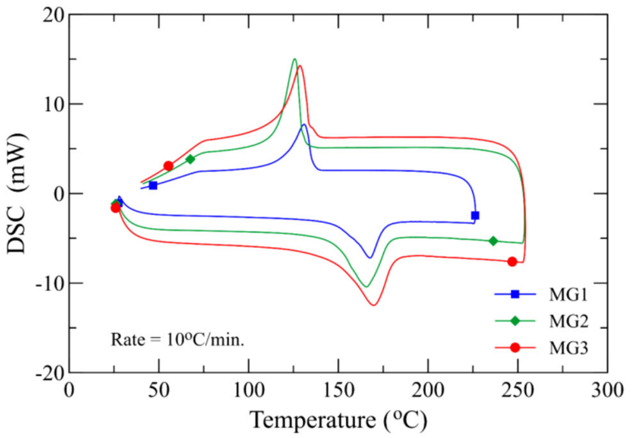

Fig. 2 DSC curves obtained at heating/cooling rate of 10 °C/min for three alloys

Table 2 Transformation temperatures and enthalpies obtained from DSC experiments with heating/cooling rate of 10 °C/min

Alloy	A_s (°C)	A_f (°C)	$\Delta H^{\mathrm{M-A}}$ (J/mol)	M_s (°C)	M_f (°C)	$\Delta H^{\mathrm{A-M}}$ (J/mol)
MG1	153.85	175.45	−423.49	136.03	119.55	443.76
MG2	147.74	178.24	−484.67	130.51	115.31	505.44
MG3	150.25	180.65	−455.28	134.55	117.21	467.50

finish temperature, A_f. Upon increasing Mg content, the forward transformation start and finish temperatures, M_s and M_f, do not change systematically. The temperature hysteresis, $\Delta T = A_\mathrm{f} - M_\mathrm{s}$, is also calculated as 39.42 °C for MG1, 47.73 °C for MG2 and 46.1 °C for MG3.

In the literature, the transformation temperatures of an alloy having nearest composition to the alloys studied here were found as 7.8 °C for M_f and 35.6 °C for A_f for $\mathrm{Cu}_{68.85}$–$\mathrm{Al}_{25.18}$–$\mathrm{Mn}_{4.87}$–$\mathrm{Mg}_{1.1}$ alloy (81.80, 12.7, 5.0 and 0.5 in wt%, respectively) [5].The Cu–Al–Mn alloys show a tendency to reduce their M_s temperature about 30 °C per 1 at% Mn increment while the Al content is kept constant [13]. It can be said that the decrease in Mn content of these alloys increases the transformation temperatures due to the forming of less stable β_1 phase. In addition, it has been reported that, in the case of Al content around 24–26 at% and the Mn content lower than 5 at%, in general, the alloys have the transformation temperatures over 100 °C, depending on ageing conditions [10, 11, 25, 32]. Although there is no considerable difference between the Al contents of the alloys used in the literature and studied here, the large differences between the transformation temperatures have been observed. The reason for the difference may be attributed to the fact that the forming of more stable β_1 phase could be suppressed by adding Mg into these alloys even if the Mn content has been raised.

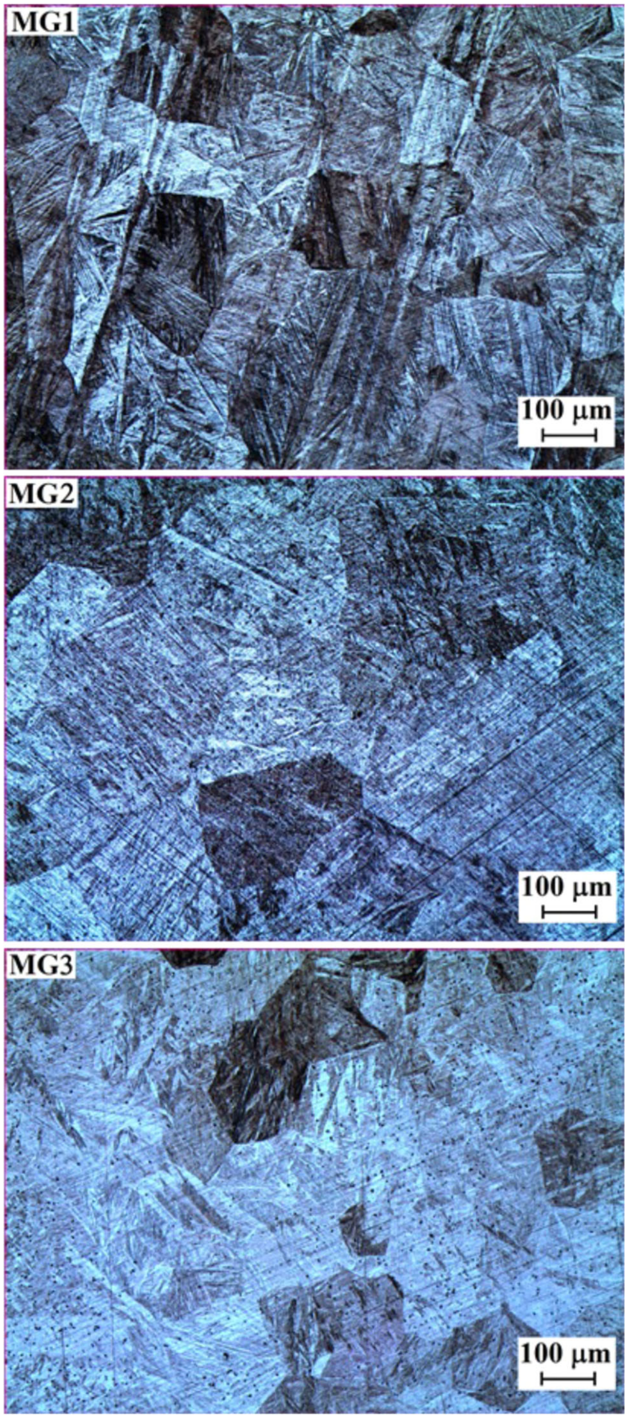

Fig. 3 Optical micrographs for three alloys in martensitic conditions

The entropy change ΔS in martensitic transformation can be calculated from $\Delta H^{\mathrm{M-A}}/T_0$ ratio, where the $\Delta H^{\mathrm{M-A}}$ is the enthalpy change given in Table 2 and the $T_0 = (A_\mathrm{f} + M_\mathrm{s})/2$ is the temperature at which the parent and martensite phases are in equilibrium. By following these definitions, the ΔS for MG1, MG2 and MG3 alloys was calculated as −0.987, −1.134 and −1.057 J/mol K, respectively. In a previous study [13], it was found that the entropy change is a constant value depending on the martensitic structure formed, and that there is an entropy difference of 0.3 J/mol K between the 2H and the 18R phases. The entropy change was also calculated as 1.264 J/mol K for 18R and 1.51 J/mol K for 2H, independent of the alloy composition used in that study [13]. The calculated values of ΔS in here are slightly lower as compared to the literature values obtained for other Cu–Al–Mn alloys, and the values of ΔS point out to the 18R-type martensites in three alloys produced here.

Optical micrographs taken at room temperature for MG1, MG2 and MG3 alloys are shown in Fig. 3. As observed in many other polycrystalline Cu–Al–Mn alloys, the alloys produced here have lath type martensitic structure at room temperature because the transformation temperatures are much higher than room temperature. From the Fig. 3, it has been seen clearly that the martensitic plates or variants, which are relatively thin with compared to other Cu–Al–Mn alloys, are formed in almost every grains. Also, as increasing Mg content the fine precipitates occur in the β phase matrix, which are shown especially for MG3, due to the low solubility of Mg in the Cu–Al–Mn alloys [5]. It is known that the precipitation hardening of these alloys leads to increase in strain constraints and a change in martensitic transformation temperatures [3, 11], which deteriorates the thermoelastic transformation characteristics.

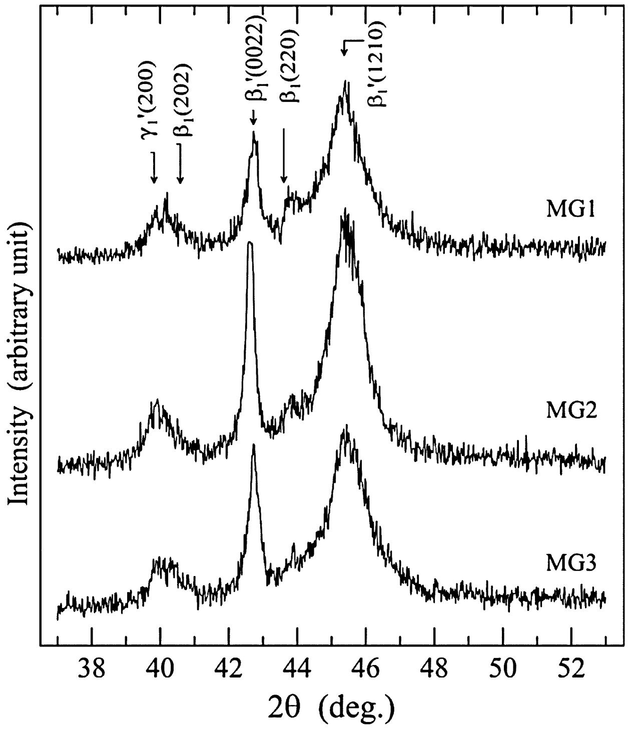

Fig. 4 XRD patterns for three alloys at room temperature

X-ray diffraction patterns at room temperature are shown in Fig. 4 for three alloys. The alloys in martensitic conditions have mainly 18R-type structure as seen from indexes of β'_1. The alloys have also some remaining of parent β phase indexed as β_1, especially shown for MG1 and MG2 alloys. It has been reported that the alloys aged at temperature above 560 °C can have 2H- and 18R-type martensites markedly [11]. 2H martensitic structure has not been observed clearly here. A little bit of γ peaks may also be marked on the X-ray pattern due to unable to prevent adequately the decomposition of β and β_1 phases to γ_2 during quenching.

4 Conclusions

The addition of trace amount of Mg into the Cu–Al–Mn shape memory alloys does not change dramatically their common characteristics. However, it can be noticed that, as lowering Mn content by replacing with Mg, the transformation temperatures have not increased as expected as in the literature [11, 13] stated that the Mn lowers the M_s temperature of Cu–Al–Mn alloys by about 30 °C per 1 % Mn. Therefore, one can say that the Mg atoms in the alloy could act a role like Mn atoms, except for the magnetic behaviour depending on spin states of atoms. Also, it has been observed that the density of fine precipitates become higher as increasing Mg content, which could affect the SME and workability of the alloys. Although, in the martensitic conditions, the Cu–Al–Mn alloys with high Al have mainly γ_1' phase structure (2H) originating from DO_3-type parent phase, the alloys produced here have mainly 18R-type structure originating from $L2_1$-type parent phase which is thought to be responsible for the ductility of the Cu–Al–Mn alloys. These findings may be supported by the calculated entropy change to be -0.987, -1.134 and -1.057 J/mol K for MG1, MG2 and MG3 alloys, respectively, which they may indicate the transformation from $L2_1$ parent to 18R-type martensites [13]. In addition, the effect of ageing temperature and time on the findings should be investigated in detail for the alloys used here due to the fact that the rapid and ageing hardening occurs in most of the Mg alloys.

References

1. K. Otsuka, C.M. Wayman, Shape memory materials. (UK: Cambridge University Press; 1999)
2. J.L. Pelegrina, M. Ahlers, The stability of the martensitic phases in Cu–Zn–Al at an electron concentration of 1.532. Acta Metal Mater **38**(2), 293–299 (1990)

3. N. Kayali, S. Ozgen, O. Adiguzel, Ageing effects on ordering degree and morphology of 18R-type martensite in shape memory CuZnAl alloys. Mater. Res. Bull. **32**(5), 569–578 (1997)
4. F.C. Lovey, V. Torra, Shape memory in Cu-based alloys: phenomenological behavior at the mesoscale level and interaction of martensitic transformation with structural defects in Cu–Zn–Al. Prog. Mater Sci. **44**, 189–289 (1999)
5. U.S. Mallik, V. Sampath, Influence of quaternary alloying additions on transformation temperatures and shape memory properties of Cu–Al–Mn shape memory alloy. J Alloys Compd **469**, 156–163 (2009)
6. V. Recarte, J.I. Pérez-Landazábal, A. Ibarra, M.L. Nó, J.S. Juan, High temperature β phase decomposition process in a Cu–Al–Ni shape memory alloy. Mater. Sci. Eng., A **378**, 238–242 (2004)
7. Z. Wang, X. Liu, J. Xie, Effects of solidification parameters on microstructure and mechanical properties of continuous columnar-grained Cu–Al–Ni alloy. Prog Natl Sci Mater Int **21**, 368–374 (2011)
8. Ş.N. Balo, M. Ceylan, Effect of Be content on some characteristics of Cu–Al–Be shape memory alloys. J. Mater. Process. Technol. **124**, 200–208 (2002)
9. R. Zengin, M. Ceylan, Influence of neutron irradiation on characteristics of Cu-13% wt.Al-4%wtNi shapememory alloy. Mater. Lett. **58**, 55–59 (2003)
10. J. Ma, I. Karaman, R.D. Noebe, High temperature shape memory alloys. Int. Mater. Rev. **55**(5), 257–315 (2010)
11. K. Matsushita, T. Okamoto, T. Okamoto, Effects of manganese and ageing on martensitic transformation of Cu–Al–Mn alloys. J. Mater. Sci. **20**, 689–699 (1985)
12. R. Kainuma, S. Takahashi, K. Ishida, Thermoelastic martensite and shape memory effect in ductile Cu-Al-Mn alloys. Metallur Mater Trans A **27A**, 2187–2195 (1996)
13. E. Obrado, L. Manosa, A. Planes, Stability of the bcc phase of Cu–Al–Mn shape-memory alloys. Phys Rev B. **56**(1), 20–23 (1997)
14. Y. Sutou, N. Koeda, T. Omori, R. Kainuma, R. Ishida, Effects of ageing on bainitic and thermally induced martensitic transformations in ductile Cu–Al–Mn-based shape memory alloys. Acta Mater. **57**, 5748–5758 (2009)
15. Q. Wang, C. Cui, Q. Wang, N. Yan, Fabrication of a porous Cu–Al–Mn shape memory alloy by the sintering-dissolution process. Mater. Lett. **65**, 2735–2738 (2011)
16. Y. Sutou, T. Omori, R. Kainuma, K. Ishida, Grain size dependence of pseudoelasticity in polycrystalline Cu–Al–Mn-based shape memory sheets. Acta Mater. **61**, 3842–3850 (2013)
17. S. Belkahla, H.F. Zuñiga, G. Guenin, Elaboration and characterization of new low temperature shape memory Cu-Al-Be alloys. Mater. Sci. Eng., A **169**(1–2), 119–124 (1993)
18. S. Montecinos, A. Cuniberti, Martensitic transformation and grain size in a Cu–Al–Be alloy. Procedia Mater. Sci. **1**, 149–155 (2012)
19. I.L. Ferreno, T. Breczewski, I.R. Larrea, A.L. Echarri, M.L. Nó, J.S. Juan, Thermal treatments and transformation behavior of Cu–Al–Be shape memory alloys. J. Alloy. Compd. **577S**, S463–S467 (2013)
20. A.T. Adorno, R.A.G. Silva, Kinetics of martensite decomposition in the Cu-9Al-6Ag alloy. J. Alloy. Compd. **402**, 105–108 (2005)
21. J.M. Guilemany, J. Fernandez, X.M. Zhang, TEM study on the microstructure of Cu–Al–Ag shape memory alloys. Mater. Sci. Eng., A **438**, 726–729 (2006)
22. Q. Wang, D. Lu, C. Cui, N. Yan, Q. Wang, Fabrication and internal friction behaviors of novel porous CuAlMn shape memory alloy filled with polystyrene. Mater. Lett. **92**, 82–85 (2013)
23. Development of a Cu-Al-Mn Shape-Memory Alloy and its Application to an Ingrown Toenail Correcting Clip. Furukawa Rev 41: 22–4 (2012)
24. Z.G. Wei, R. Sandsrom, S. Miyazaki, Shape-memory materials and hybrid composites for smart systems: Part I Shape-memory materials. J. Mater. Sci. **33**, 3743–3762 (1998)
25. Y. Sutou, T. Omori, R. Kainuma, K. Ishida, Ductile Cu–Al–Mn based shape memory alloys: general properties and applications. Mater. Sci. Technol. **24**(8), 896–901 (2008)
26. R. Kainuma, N. Satoh, X.J. Liu, I. Ohnuma, K. Ishida, Phase equilibria and Heusler phase stability in the Cu-rich portion of the Cu-Al-Mn system. J. Alloy. Compd. **266**, 191–200 (1998)
27. E.S. Gouda, E. Ahmed, N. Tawfik, Melting and corrosion behavior of Al-9Zn based alloys with Cu and Mg additions. Mater. Sci. Appl. **2**, 469–475 (2011)
28. Z.Q. Zheng, W.Q. Liu, Z.Q.Liao, S.P. Ringer, G. Sha, Solute clustering and solute nanostructures in an Al-3.5Cu-0.4 Mg-0.2Ge alloy. Acta Materialia.http://www.sciencedirect.com/science/journal/13596454/61/10 61(10): 3724–34 (2013)
29. M.M. Rahvard, M. Tamizifar, S.M.A. Boutorabi, S.G. Shiri, Characterization of the graded distribution of primary particles and wear behavior in the A390 alloy ring with various Mg contents fabricated by centrifugal casting. Mater. Des. **56**, 105–114 (2014)
30. S.D. Kulkarni, Thermodynamics of martensitic and eutectoid transformations in the Cu-Al system. Acta Metall. **21**, 1461–1469 (1973)
31. E. Obrado, C. Frontera, L. Manosa, A. Planes, Order-disorder transitions of Cu–Al–Mn shape-memory alloys. Phys. Rev. B. **58**(21), 14245–14255 (1998)
32. M.O. Prado, Martensitic transformation in a mictomagnetic Cu–Al–Mn alloy. Scripta Mater. **44**, 2431–2436 (2001)
33. R.A.G. Silva, A. Cuniberti, M. Stipcich, A.T. Adorno, Effect of Ag addition on the martensitic phase of the Cu–10 wt% Al alloy. Mater. Sci. Eng., A **456**, 5–10 (2007)